Visualizing and Exploring Higher-Order Dependencies in Complex Systems

JUN TAO, University of Notre Dame
JIAN XU, Citadel LLC
CHAOLI WANG, University of Notre Dame
NITESH V. CHAWLA, University of Notre Dame

Unlike the conventional first-order network (FoN), the higher-order network (HoN) provides a more accurate description of transitions by creating additional nodes to encode higher-order dependencies. However, there exists no visualization and exploration tool for HoNs. For applications such as the development of strategies to control species invasion through global shipping which is known to exhibit higher-order dependencies, the existing FoN visualization is limited. In this paper, we present HoNVis, a novel visual analytics framework for exploring higher-order dependencies that reside in various kinds of complex systems. Our framework leverages coordinated multiple views to reveal the network structure at three levels of detail (i.e., the global, local, and individual node levels). Users can quickly identify nodes of interest at the global level and specify a first-order node to investigate its higher-order nodes at the individual node level. A larger-scale impact can be further investigated through the exploration of HoN at the local level. In addition, comparative visualization is enabled for each view to understand the dynamic behaviors of a series of HoNs. We demonstrate the effectiveness of our approach using two real-world applications, the global shipping network and the New York City taxi trips, with use cases conducted by domain experts.

CCS Concepts: • **Information systems** → *Geographic information systems*; • **Human-centered computing** → **Visual analytics**; • **Computing methodologies** → *Knowledge representation and reasoning*;

Additional Key Words and Phrases: Higher-order dependencies, networks, sequential data, visual analytics.

ACM Reference Format:
Jun Tao, Jian Xu, Chaoli Wang, and Nitesh V. Chawla. 2018. Visualizing and Exploring Higher-Order Dependencies in Complex Systems. *ACM Trans. Interact. Intell. Syst.* 1, 1 (July 2018), 25 pages. https://doi.org/0000001.0000001

1 INTRODUCTION

Modern day systems are complex, whether they are movements of hundreds of thousands of ships to form a global shipping network [17], powering the transportation and economy while inadvertently translocating invasive species; interactions of billions of people on social networks, facilitating the diffusion of information; or complex metabolic systems representing rich cellular interactions.

The complex systems are often represented as networks, where the components of the system are represented as nodes and the interactions among them are represented as edges or links. This

Authors' addresses: Jun Tao, University of Notre Dame, Department of Computer Science and Engineering, jtao1@nd.edu; Jian Xu, Citadel LLC, i@jianxu.net; Chaoli Wang, University of Notre Dame, Department of Computer Science and Engineering, chaoli.wang@nd.edu; Nitesh V. Chawla, University of Notre Dame, Department of Computer Science and Engineering, nchawla@nd.edu.

2160-6455/2018/7-ART $15.00
https://doi.org/0000001.0000001

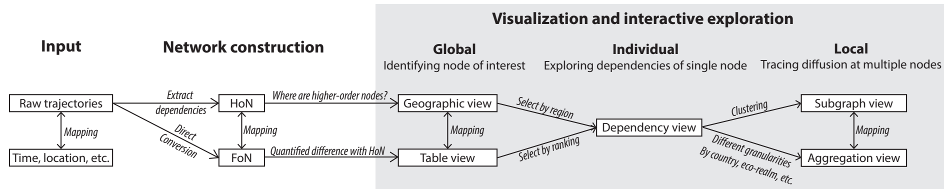

Fig. 1. The framework of HoNVis design. FoN and HoN are converted and extracted from the raw trajectory data, from which we identify nodes of interest. Five linked views are designed to enable the interrogation of single and multiple nodes.

network based representation facilitates subsequent analysis and visualization. For example, the global shipping activities are usually represented as a global shipping network, with ports as nodes, and the amount of traffic between port pairs as edge weights [19]. Traditionally, creating networks from such ship movement data has followed the port-to-port movement of a ship, and ignores the historic trajectory of the ship. This becomes extremely limiting as it has been observed that ship movements actually depend on up to *five* previously visited ports [36]; other types of interaction data from communication to transportation often exhibit *higher-order dependencies* [9, 28]. Therefore, when representing data derived from these complex systems, conventional network representations that implicitly assume the Markov property (i.e., *first-order dependency*) can quickly become limiting, undermining subsequent network analysis that relies on the network representation.

To address this problem, prior work has proposed the use of *higher-order network* (HoN) to discover higher-order dependencies and embed conditional transition probabilities into a network representation [36]. For the global shipping network example, instead of mapping every port to a single node, each higher-order node in HoN encodes not only the current step (the port that a ship currently stays) but also a sequence of previous steps (the ports that a ship visited before arriving at the current port). Therefore, the transitions among nodes in a HoN are now conditional, and are able to reproduce complex ship movement patterns more accurately from the raw data. HoN features direct compatibility with the existing suite of network analysis methods, such as random walking, clustering, and ranking, thus serving as a powerful tool for modeling the increasingly complex systems.

HoN is the correct way of representing complex systems that defy the first-order dependency assumptions. Despite the importance of HoN and its applicability to network analysis, there has not yet been a visualization tool that can handle the richness of the HoN representation. In this paper, we present a visual analytics framework, named HoNVis, to facilitate the exploration and understanding of both steady and dynamic and HoNs. Two applications, namely, the global shipping network and the taxi trip data, are used to guide the development of our framework and examine its effectiveness.

The global shipping network, being an important application of HoN for the study of invasive species, is used as a case study and for illustration throughout this paper. Since the shipping network is sparse in time, we construct a single HoN for analysis. We team up with two domain experts in network science and marine ecology and develop HoNVis. We focus on the formation and impact of higher-order nodes, e.g., why a higher-order node exists in a HoN and how the species may propagate from a port to other ports given the previous steps? Specific to the shipping network case study, we aim to answer these questions through a three-step exploration process: (1) *global identification of ports of interest*, (2) *detailed observation of the connections of an individual port*, and (3) *tracing the propagation of invasive species from port to port through shipping*. Accordingly, we lay out the design of HoNVis in Figure 1. The input data are converted to the FoN and dependencies are extracted to construct the HoN. From these network representations, we identify nodes of interest. The visualization includes five coordinated views: *geographic view* and *table view* show information related to a single node; *dependency view*, *subgraph view*, and *aggregation view* show connections among multiple nodes. Together these five views enable users to explore higher-order nodes and their dependencies, allowing insights to be gained from this comprehensive system.

Our second application uses the taxi trip data where we construct a sequence of HoNs to study the dynamic behaviors of higher-order dependencies. Other than identifying points of interest (POIs), exploring the connections, and analyzing the propagation pattern through taxi traffic, we further investigate how the travel patterns through taxis may vary on different days. We demonstrate that the abnormal patterns, caused by events or extreme weather conditions, can be identified using the New York City taxi trip data in 2013.

2 RELATED WORK

HoN Visualization. HoN visualization is sporadic in the literature. Blaas et al. [5] proposed to visualize higher-order transitions by connecting nodes using higher-order curves. By following a smooth curve from one end to the other, one can identify which nodes are associated with higher-order transitions and what are the orders of the nodes. Rosvall et al. [28] grouped higher-order nodes by their current nodes and drew directed edges between connected nodes. The higher-order nodes representing the same physical locations are placed in one circle to build the correspondence. This approach, although intuitive, does not scale beyond the second order, nor when more than a dozen of higher-order nodes representing the same location coexist. HoN is also used as an analysis tool in unsteady flow visualization for better workload distribution. Zhang et al. [38] employed high-order dependencies to estimate the destinations of particles given their previous locations, providing more accurate information about which data blocks to load at the next step.

Visual Analytics of Temporal Event Sequences. Although HoN is less explored in the field of visualization, our target data, temporal event sequences have been extensively studied in previous work. Wongsuphasawat et al. [34] presented LifeFlow to study and compare multiple event sequences. Based on events, the sequences are aggregated to form a tree for an overview. Detailed event information for each sequence is displayed as a list. Wongsuphasawat and Gotz [35] extended LifeFlow and developed Outflow, which aggregates sequences to form a graph to further reduce the number of events presented in the overview. The aggregated sequences are visualized using the Sankey diagram. Liu et al. [22] proposed CoreFlow, which extracts the core events in sequences and creates a tree using the core events as nodes. The branching structure of the tree summarizes the sequences for users to understand the general pattern. Bodesinsky et al. [7] proposed an interface with coordinated multiple views to explore sequences of events. The event view visualizes each sequence of events as horizontally aligned bars. Event patterns are summarized in a pattern overview from which users can query a certain pattern to highlight the recurring instances in the event view. Partl et al. [27] designed Pathfinder to analyze paths in multivariate graphs. In their work, a node-link diagram visualizes the paths between queried nodes, and a ranked list shows the attributes associated with the nodes. Chen et al. [8] summarized event sequences based on the minimum description length principle. The extracted patterns minimize the summation of pattern lengths and the number of corrections needed to edit the sequences into the patterns.

The aforementioned techniques tackled two major challenges of visualizing event sequences: the volume of data and the variety of patterns. Du et al. [11] surveyed the methods for addressing both challenges. They described 15 strategies which fall into four groups: extraction, temporal folding, pattern simplification, and iterative strategies. Malik et al. [24] proposed high-volume hypothesis testing to compare two groups of sequences. The statistics information is derived and presented to users for visual comparison of the same sequences in the two groups. Similar to our work, Steptoe et al. [31] studied user trajectories in theme parks by converting them into event sequences. Each sequence is visualized as a bar where the events are colored differently to indicate the time spent on different locations.

Unlike these works, our work has a fundamentally different goal: instead of discovering the patterns in the sequences, we focus on extracting high-order dependencies among the events by identifying sub-sequences that exhibit different transition patterns. We further synthesize the sub-sequences and their transition probabilities to form a HoN, where the traditional graph and network analysis tools can be directly applied. This allows us to study not only sequence patterns but also large-scale behavior (e.g., diffusion).

Movement Data Visualization. Spatiotemporal movement data (e.g., traffic and trajectory) are often encoded as conventional graphs, where each node represents a location and an edge represents the traffic volume between two locations without distinguishing their previous locations. Guo [14] used the location-to-location graph to visualize population migration in the United States. The spatial regions are partitioned to form hierarchies and support node aggregation at the regional level. The flow is clustered based on the associated variables, such as the number of migrants for different ages and income levels. von Landesberger et al. [32] presented the MobilityGraph to visualize mass mobility. They also grouped the regions for clearer observation. To obtain a common movement pattern, a temporal clustering is performed based on the graph's feature vectors generated in different time spans. However, both works do not consider higher-order dependencies and therefore, they are not able to answer the questions such as how many migrants in Chicago who came from Los Angles would finally move to New York City.

3 HIGHER-ORDER NETWORK ALGORITHM

Networks are commonly used to describe transitions in sequential data. The conventional approaches usually assume Markov property (i.e., first-order dependency) and construct FoNs that only synthesize the transitions between neighboring states in sequences. However, it has been shown that higher-order dependencies exist ubiquitously in flow dynamics such as ship movements, air traffic, and web clickstreams [4, 9, 28], which renders the conventional approaches limited. In this section, we start with a brief description of FoN and then introduce the concept and construction of HoN following the approach proposed by Xu et al. [36]. We use one example from the global ocean shipping to motivate the use of HoN through comparison with FoN.

Conventional FoN. The conventional approach to constructing a network from the raw data is to count the numbers of observed interactions between entities as the edge weights between node pairs. For example, given the observed ship movements shown in Figure 2 (a), a conventional shipping network is constructed as shown in Figure 2 (b), with every node representing a port and every edge representing the amount of traffic between a pair of ports. Since only direct movements are preserved in the network structure as pairwise connections, this approach implicitly assumes the Markov property, i.e., a ship's probability of moving from the current port i_t to the next port i_{t+1} is proportional to the edge weight $w(i_t \longrightarrow i_{t+1})$:

$$p(X_{t+1} = i_{t+1} | X_t = i_t) = \frac{w(i_t \longrightarrow i_{t+1})}{\sum_j w(i_t \longrightarrow j)}. \tag{1}$$

In the example of Figure 2 (b), a ship is equally likely to move to ports X and Y from port M, regardless of from where the ship coming to M. However, from Figure 2 (a), it is apparent that ships coming from A to M are more likely to go to X, and ships coming from B to M are more likely to go to Y. Such important information about higher-order dependencies is lost using the conventional approach.

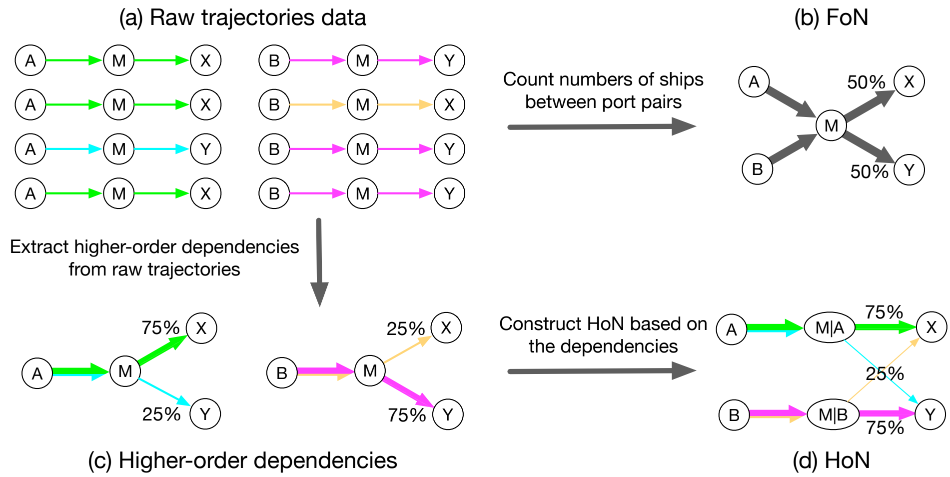

Fig. 2. (a) An example of raw trajectory data. (b) Construction of the FoN from raw trajectory data. (c) Extraction of higher-order dependencies from raw trajectories. (d) Construction of the HoN from higher-order dependencies.

Construction of HoN. HoN representation captures arbitrary higher-order dependencies by considering each higher-order node $\boldsymbol{i}_t$ to be a sequence of entities (such as ports), i.e., $\boldsymbol{i}_t = [i_t|i_{t-1}, i_{t-2}, \dots]$. In this way, the transition probability in HoN describes the movements between sequences

$$p(X_{t+1} = [i_{t+1}|i_t, i_{t-1}, \dots]|X_t = [i_t|i_{t-1}, i_{t-2}, \dots]) = \frac{w([i_t|i_{t-1}, i_{t-2}, \dots] \rightarrow i_{t+1})}{\sum_j w([i_t|i_{t-1}, i_{t-2}, \dots] \rightarrow j)}. \qquad (2)$$

By encoding the additional information of previous entities in a higher-order node, we capture the higher-order dependencies among entities. To reduce the number of higher-order nodes for scalability, unnecessary higher-order nodes, which behave similarly as their corresponding lower-order nodes, are removed. As illustrated in Figure 2 (c), in the context of global shipping, the method first evaluates the transition probability from the higher-order node $M|A$ to a port X and port Y. Then, it evaluates if knowing the ship came from A to M (i.e., $M|A$) significantly changes the probability distribution of the ship's next step from M. If the change, as measured by the Kullback-Leibler divergence (KLD) [21], is significant, as the case shown in Figure 2, it suggests that the ship movements depend on not only the current port M but also the previous port A. This comparison is iterated recursively to extract higher-order dependencies. Next, in the network representation, instead of mapping every port to a single node, every node represents the current port given a short sequence of previous ports. For example, in Figure 2 (d), the port M is now broken down into two higher-order ports $M|A$ and $M|B$, such that ships coming from different ports to M can have different probability distributions of choosing the next port to visit.

How Does HoN Influence Network Analysis? An important property of HoN is that its data structure—nodes connected by edges—is consistent with the conventional FoN (the only difference is node labeling), making HoN directly compatible with the whole existing network analysis toolkit. When ship movements are simulated on HoN as random walking, the transition probabilities between sequences of ports preserve the higher-order dependencies among ports. Therefore, although the transition (Equation 2) appears to be Markovian, arbitrary orders of dependencies can be incorporated into the equation, refining the patterns of the simulated ship movement. This flexibility of HoN to embed *variable orders*, on the other hand, brings new challenges to visualization as there can be tens to hundreds of nodes of variable orders representing the same physical port.

The HoN, being a more accurate representation of flow dynamics in the raw data, serves as a better foundation of subsequent network analysis. By following the auxiliary higher-order nodes and edges, random walkers on the HoN representation of global shipping demonstrate at least *twice* the accuracy on simulating the actual ship movements than on the FoN [36]. Furthermore, while the movement flows are "memoryless" and are mixed in every step on a FoN, on the HoN the flows are more clearly distinguished. That is, random walkers on the HoN have higher certainty in making every step, leading to significantly lower *entropy rates* [28, 36]

$$H(X_{t+1}|X_t) = -\sum_{\boldsymbol{i},\boldsymbol{j}} \pi(\boldsymbol{i}) p(\boldsymbol{i} \rightarrow \boldsymbol{j}) \log p(\boldsymbol{i} \rightarrow \boldsymbol{j}), \tag{3}$$

where $\pi(\boldsymbol{i})$ is the stationary distribution at node $\boldsymbol{i}$ and $p(\boldsymbol{i} \rightarrow \boldsymbol{j})$ is the transition probability from node $\boldsymbol{i}$ to node $\boldsymbol{j}$ as computed in Equation 2. The changes of random walkers' behavior on the HoN also influence the results of important network analysis methods such as PageRank [26] for ranking, which relies on random walkers to simulate movements in the network. For example, these clustering methods are based on the intuition that a random walker is more likely to move within the same cluster rather than between different clusters. In the HoN shown in Figure 2 (d), port X receives more traffic from port A than from port B, thus X and A are more likely to be clustered together. On the contrary, in the FoN shown in Figure 2 (b), A and B appear to be equivalent to X, regardless of the indirect flow patterns. For the study of invasive species, the clustering result on HoN provides more insight, since port X is more susceptible to species originating from A carried via indirect shipping.

4 DESIGN RATIONALES

4.1 Application Background

Global Ocean Shipping Network. The global shipping network is the dominant vector for the unintentional introduction of invasive species [25]: species "hitchhike" on ships from port to port in ballast water or via hull fouling [10]. Understanding the global shipping network is crucial for devising species control management strategies. The data mining community has recently produced promising observations on the global shipping network [37]. However, even the state-of-the-art research still faces unresolved challenges. It is unclear from the FoN how species may propagate after multiple steps, and it is impossible to know which port or pathway plays an important role connecting different clusters, eco-regions, or countries. Although it has been shown how ship types, ship sizes, geographical locations and seasonality can influence the structure of the first-order global shipping and species flow patterns, there has been no discussion on how such factors influence higher-order shipping patterns. It is unknown whether higher-order movement patterns are mainly formed by oil tankers, or located at estuaries, or appear mainly in winters. Such information can provide insight in revealing the driving forces behind the formation of higher-order dependencies in ship movements, and aid the development of invasive species management strategies.

New York City Taxi Trips. Taxi trip data have been visualized and analyzed to study movement patterns in cities [13, 16]. Understanding these higher-order dependencies of taxi trips will help urban planners design transportation systems, advertising managers identify billboard locations, and social scientists understand lives in a city, etc. For example, the higher-order dependencies can better capture the multi-step movement patterns among POIs, which may assist the design of touring bus routes. We may use HoNs to precisely model the propagation of flu through taxis as well. This can lead to more effective flu control policies. However, the dynamic behaviors of the higher-order dependencies are never investigated in the taxi trip application. It is unknown whether or not the higher-order travel patterns through taxis would change over time or when an abnormal multi-step movement pattern would appear.

4.2 Design Requirements

Given the gap between the demand for visualizing higher-order dependencies and the lack of HoN visualization tools, we first identify key requirements for our visual analytics system to explore a single HoN (**R1** to **R4**) and then discuss the additional requirements for exploring dynamic HoNs (**R5** and **R6**).

R1. Create a mapping between the HoN and FoN, and quantify the differences. The experts expect to see geographical locations of ports and their connections on a map, in order to select ports at places of interest; the experts want to know if higher-order dependencies are more likely to exist in certain geographical locations (e.g., canals and straits). Additionally, the experts expect to learn how do the FoN and HoN representations compare with each other in terms of network properties such as port centralities.

While the HoN contains richer information, the FoN has the simplicity of one-to-one mapping from nodes to geographical locations on a map. To combine the advantage of both representations, we map the structure of HoN back to the FoN when visualizing it on the map, and assign scalar values to the corresponding nodes and edges in the FoN for comparison. The comparison can be defined in multiple ways depending on the exploration goal. By default, we quantify the difference of the transition probabilities between the HoN and FoN. The difference can also be quantified by comparing the network analysis results. For example, domain experts are interested in the nodes with the largest PageRank [26], which effectively simulate the flow of invasive species; the PageRank differences can help to identify ports with underestimated risks in FoN. In brief, mapping the difference or important values to FoN provides clearer observation on the map view and allows users to effectively identify and select the regions of interest for further exploration.

R2. Provide aggregation view of the higher-order nodes. The experts would like to explore port connections at different granularities, such as connections among countries, continents, eco-regions, eco-realms, etc. Therefore, the higher-order nodes should be aggregated and visualized for high-level knowledge discovery. For example, it should provide information such as how many nodes with the highest order exist in an eco-realm (to reveal geographical distribution of higher-order dependencies), how many pathways incorporated in higher-order nodes navigate through multiple eco-realms (to identify non-indigenous species diffusion pathways), and so on. The level of aggregation should be flexible so that users can observe the connections at different granularities, such as countries, continents, eco-regions, eco-realms, temperature and salinity ranges, etc.

R3. Visualize higher-order dependencies associated with a given port. The experts first want to know that given a port, *how* do the previous steps change a ship's choice of the next step. For example, ships currently at Singapore may have equal probabilities of going to Los Angeles and Seattle. The experts wonder if ships coming from certain ports to Singapore will make them more likely go to Los Angeles, and how much the difference is. Meanwhile, the experts want to know if certain features correlate with the existence of higher-order dependencies. For example, are higher-order dependencies mainly associated with certain types of ships (such as oil tankers), or certain geographical locations (such as canals)?

Therefore, when a port of interest is designated, a subgraph of HoN containing all higher-order nodes and edges associated with the port of interest should be generated. The transition probabilities from different higher-order nodes to the next node should be represented, in order to show how the previous ports a ship has visited may influence the ship's next step. Additionally, the attributes

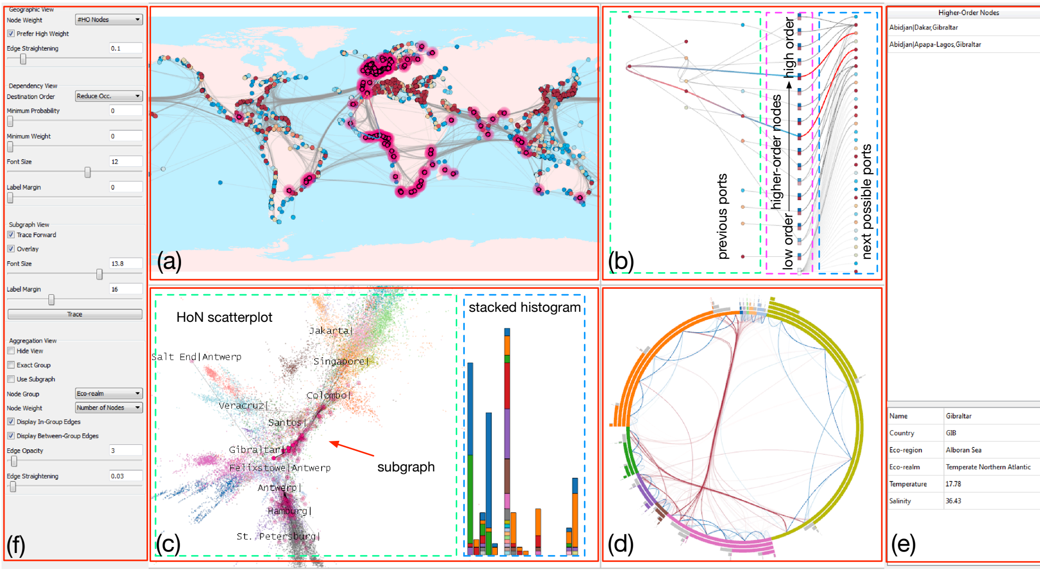

Fig. 3. The overview of HoNVis, our visual analytics system for exploring the global shipping higher-order network. (a) Geographic view. (b) Dependency view. (c) Subgraph view. (d) Aggregation view. (e) Table view. (f) Parameter panel.

of ships corresponding to the transitions should be shown, such that users may discover certain higher-order movement patterns exclusively associated with certain types of ships, particular months, and so on. For example, if the ships moving between two ports are mostly passenger ships, the ship is likely to return to the previous port, since passenger ships are likely to move between two ports instead of among multiple ports. Therefore, we should encode these attributes associated with transitions, so that once transitions of interest are identified, users can observe the corresponding attributes.

R4. Visualize and expand a subgraph. In the context of invasive species studies, the experts hope to see if higher-order dependencies are evenly distributed in the network or only exist in certain groups of tightly connected ports. The experts also expect to visualize and expand a subgraph of invaded ports to understand how invasive species propagate from a given port. The expansion should be performed forward or backward to cover more nodes along paths of interest. This allows interactive exploration and facilitates case studies on studying the species flow along certain shipping pathways. To understand the influence of these paths to the entire network, such as which are the important pathways that connect different clusters of ports, visual connections should be established between the subgraph and the entire network.

However, synthesizing all the sequential data into a single HoN cannot capture the dynamic behaviors of the underlying data. For example, a single HoN fails to answer such questions: is it always the case that a ship at port A coming from B will be more likely to visit C than D (i.e., $p(A|B \rightarrow C) > p(A|B \rightarrow D)$)? Will an existing higher-order dependency disappear at some time? To investigate this kind of dynamic higher-order dependencies, we use multiple HoNs with each encoding the sequential data within a time window, and further identify the requirements for visually exploring dynamic HoNs.

R5. Visualize the difference between multiple HoNs. The experts would like to inspect the overall difference between multiple HoNs: given a sequence of HoNs, they expect to identify the "change point", when a HoN starts to exhibit different behaviors from the preceding HoNs; and, given a certain HoN, they want to know which HoNs behave similarly and which ones behave differently. Through this inspection, the experts expect to discover the temporal evolution pattern of the networks. For example, is the current movement pattern of ships similar to that in the last decade, or is the movement pattern in summer the same as that in winter? Therefore, we should quantify the difference between two HoNs and visualize the difference among the HoNs to guide the exploration.

R6. Enable detailed comparison between two HoNs. The experts want to compare two HoNs at the individual node, aggregation, and subgraph levels, analogous to the exploration of a single HoN. For a given port, the experts expect to distinguish the higher-order dependencies shared by the two HoNs from the ones that appear in only one HoN. At the aggregation level, the experts would like to understand the difference between higher-order dependencies at coarser granularities. At the subgraph level, the experts want to know how the propagation patterns differ from each other when starting from the same set of nodes in two different HoNs. Therefore, we should extend the design of our visualization and exploration for the single HoNs to enable visual comparison.

5 SYSTEM DESCRIPTION

We design five coordinated views to meet the design requirements stated in Section 4. The five views of our HoNVis are: (1) a *geographic view* where the geographical locations of ports and the connections among them are displayed; (2) a *dependency view* that shows all the higher-order nodes associated with a given port, as well as the previously visited ports and the next possible ports to visit (Section 5.1); (3) a *subgraph view* that compares a user-generated subgraph with the graph showing the entire HoN (Section 5.2); (4) an *aggregation view* that visualizes higher-order dependencies under a certain aggregation criterion (Section 5.3); and 5) a *table view* that displays the detailed text information of a port or the current user exploration status. Users can hide the aggregation view to leave more vertical space for the dependency view. All these five views are linked together through brushing and linking. Labels of higher-order nodes/ports will be shown in the dependency view and subgraph view, since they cannot be inferred from the respective layout.

With HoNVis, a typical user workflow is as follows. Users start from the geographic view and aggregation view. In the geographic view, they identify through visual encoding (red to gray to blue for high to medium to low), the ports with more higher-order nodes or ports whose rankings change the most in the HoN compared to the FoN. In the aggregation view, both the current nodes and their previous steps are aggregated according to a given criterion. For example, when the entire network is aggregated at the eco-realm level, users can efficiently identify the higher-order nodes whose previous steps contain ports in other eco-realms, suggesting non-indigenous species introduction pathways. Users may then specify a port for individual port investigation: all higher-order nodes containing pathways leading to the given port will be visualized in the dependency view, showing how ships or species coming from different pathways to the current port will have different probability distributions of choosing the next port. Assuming a potentially invasive species in the current port, users can also trace species diffusion in the subgraph view, and understand how the species may propagate to different clusters of ports. Starting from the higher-order nodes directly related to the specified port, users can expand the subgraph of invaded ports by tracing forward or backward and including the nodes visited. This stepwise expansion gradually fills the gap between the one-step neighborhood of the selected port and the entire global shipping network, which helps users evaluate the impact of a port or a higher-order node at a larger scale. After each user operation, we use animated transition to emphasize the changes in other views, indicating where to explore in the next step. In the following, we describe the dependency view, subgraph view, and aggregation view in the setting of a single HoN using the global shipping network scenario. The other two views (refer to Figure 3 (a) and (e)) are omitted as their design and roles are straightforward. Then, we extend the framework to dynamic HoNs by adding a time slider (refer to Figure 6 (c)) to select HoNs and introducing comparative visualization components to compare two HoNs. The extension is described in the scenario of taxi traffic network. In this section, we will use ports or POIs to refer to first-order nodes in the global shipping and taxi traffic scenarios, respectively.

5.1 Dependency View

Given a set of higher-order nodes, the dependency view shows the connections among previously visited ports and next possible ports to visit. It corresponds to the design requirements **R1** and **R3**. The higher-order nodes being investigated can be the higher-order nodes associated with a port selected in the geographic view, or multiple higher-order nodes contained in an aggregated node selected in the aggregation view. The transitions between the higher-order nodes and their next possible ports can be filtered by the probabilities or the number of ships associated with the transitions. This produces a compact visualization allowing the more important transitions to be observed clearly. A set of attributes is assigned to the ports, providing visual hints to guide the exploration. These attributes include computed ones (e.g., PageRank in the FoN, aggregated PageRank in the HoN, and the number of associated higher-order nodes) and the geographical properties (e.g., temperature, salinity, and eco-realm).

Higher-Order Nodes. Each higher-order node is displayed as a rectangle, as shown in Figure 3 (b). Each rectangle is divided into two boxes: the upper and lower boxes. The upper box indicates the entropy of transition probabilities starting from the higher-order node, where blue/white corresponds to low/high entropy (*low* entropy corresponds to *high* certainty). The lower box indicates the KLD of the transition probability distributions of the higher-order node and its corresponding first-order node, where red/white corresponds to high/low KLD. These two properties are of particular interest, since the first one represents the *certainty* of the next port to visit given the higher-order dependency and the second one represents the *difference* between the higher-order node and its corresponding first-order node. Therefore, distinct higher-order patterns significantly different from first-order ones show a combination of blue and red boxes and can be identified at a glance. In Figure 3 (b), we observe considerable blue/red combinations, indicating higher-order dependencies of potential interest that are not captured in the FoN. Higher-order nodes with high entropy or low KLD values, though less interesting by themselves, are indispensable for bridging the connection of other higher-order nodes.

If the number of higher-order nodes is large, we only display the lower KLD boxes of nodes, since KLD is the deciding factor for extracting higher-order dependencies and is more relevant to the formation of higher-order nodes. The higher-order nodes are lined up according to their current ports and orders: the nodes with the same current port are contiguous and the node with highest/lowest order is placed at the top/bottom of that contiguous space.

Previous Ports. We display the previous ports as circles to the left side of the higher-order nodes, as shown in Figure 3 (b). For each higher-order node, we draw a smooth high-order Catmull-Rom spline to connect its corresponding ports in the visit order for clear observation, as suggested by Blaas et al. [5]. The curves exhibit color transition from red to blue, indicating the visit order of ports (i.e., red indicates the port visited first and blue indicates the current port).

We determine the layout of the previous ports using a simple heuristic: their x-coordinates are determined by their earliest appearance in any higher-order nodes; and their y-coordinates are determined by the average y-coordinates of the higher-order nodes containing them. The ports that are placed at the same locations are moved vertically to resolve the conflict. In Figure 3 (b), we

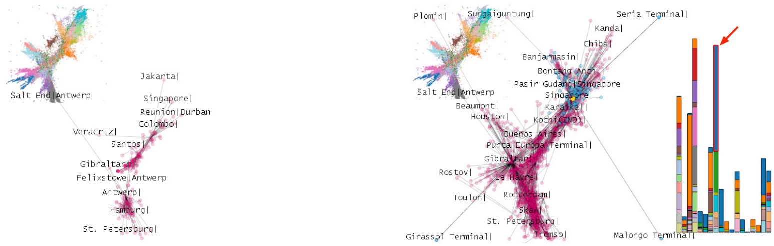

(a) (b)

Fig. 4. The subgraph view. (a) HoN scatterplot and subgraph. (b) HoN scatterplot, subgraph expanded from the subgraph shown in (a), and stacked histogram showing node contribution.

find that the ports are aligned from left to right in their visit order for most higher-order nodes. The ports associated with individual second-order nodes are mostly placed at the lower part of the dependency view and the ports associated with more higher-order nodes are mostly placed at the upper part. More sophisticated algorithms exist for drawing directed graphs, but they tend to increase the horizontal span in order to better preserve the order of nodes, which may not be ideal in our scenario given the limited screen space.

Next Possible Ports. We display the next possible ports as circles to the right side of the higher-order nodes, as shown in Figure 3 (b). The opacity of an edge connecting a higher-order node and a next possible port indicates the corresponding transition probability. In Figure 3 (b), since most edges associated with higher-order nodes are dark, their next steps to take are fairly certain. Furthermore, the edges associated with the first-order node at the bottom share similar light colors, which indicates that the next possible ports will be visited with similar probabilities.

The next possible ports can be lined up to reduce edge crossing or reflect a user-specified property. To reduce edge crossing, we first estimate the y-coordinate of a port using the average y-coordinates of the higher-order nodes connecting to that port weighted by their respective transition probabilities. Thus, a port will be placed closer to the higher-order nodes that are more likely to transit to it. Then, all ports are evenly spaced to span the entire screen space along a vertical line, preserving their estimated y-coordinates. Users can also arrange the ports according to an associated property. This facilitates the identification of transitions related to certain characteristics (e.g., high temperature or a certain eco-realm).

Interaction. Users can select a previous port in the dependency view for investigation. The curves associated with that port will maintain their colors, while the other curves will become gray. In the table view, we display the names of the higher-order nodes containing the selected port and the information of this port. In the subgraph view, the subgraph will be updated as well, so that users can study the propagation pattern given that port as a previous node. Users can further select a set of next possible ports. To provide detailed information, we display two histograms of ship types and temporal activities of the transitions between the selected higher-order nodes and the next possible ports.

5.2 Subgraph View

The subgraph view visualizes a subgraph of the HoN in the context of the entire network, corresponding to the design requirement **R2**. It shows the topological proximity of ports, and allows users to expand the subgraph of invaded ports to explore how the invasive species will propagate over the network. The entire HoN is described by a layout of the network using ForceAtlas2 [18].

Meanwhile, the structural organizations of HoN also influence the propagation dynamics. For example, the global shipping network is naturally organized into multiple communities; in each community the ports are tightly coupled by shipping traffic. Once a given species is introduced to a community, the species will propagate through the whole community shortly. Therefore, locating the *entry points* and *pathways* to communities is essential to devising species control strategies. We apply the widely-used Louvain method [6] for community detection, using edge weights and the default resolution of 1.0. Note that higher-order nodes representing the same port could belong to different communities, which naturally yield overlapping clusters and indicate how certain ports may be susceptible to multiple sources of species invasion.

We visualize the entire HoN using scatterplot, where each point represents a node in HoN, colored by the community of that node. The edges in the HoN are ignored for clutter reduction. The subgraph is then displayed on top of the scatterplot. Each node in the subgraph is drawn as a semi-transparent circle, whose center is placed at the corresponding point in the scatterplot. The transparency of a circle indicates the probability of the corresponding node being reached during the expansion of the subgraph. An edge in the subgraph is drawn as a straight line with transparency indicating the corresponding transition probability. In Figure 3 (c), the subgraph expanded from the two higher-order nodes selected in the dependency view is displayed on top of the HoN scatterplot. We can see that the subgraph mostly covers the lower right branch and the lower middle region of the network. As an option, users can choose not to overlay the subgraph and the HoN scatterplot. In that case, the HoN scatterplot will be displayed in the top-left corner of the subgraph view, as shown in Figure 4 (a). Without the overlay, the nodes in the subgraph can be observed more clearly, but the covered regions can only be roughly interpreted.

Subgraph Expansion. Subgraph expansion is performed by tracing from the nodes in the current subgraph and including the nodes reached during the tracing. Users can trace backward to find out through which nodes the subgraph can be reached or trace forward to explore the nodes that will be reached from the nodes in the current subgraph. The subgraph expansion procedure starts from a set of higher-order nodes selected in the other views. The initial probability of reaching a node is proportional to the number of ships leaving/arriving that node when tracing forward/backward. After each tracing step, the probability of reaching a node n_i will be updated to $\sum_{n_j \in N(n_i)} p(n_j)p(e_{ji})$, where $N(n_i)$ is the set of nodes from which n_i will be reached, $p(n_j)$ is the probability of n_j being reached, and $p(e_{ji})$ is the transition probability from n_j to n_i. The expansion can be observed in both the HoN scatterplot and the geographic map, where the ports associated with any node in the subgraph is highlighted. A tracing step is only performed when users click the "Trace" button in the parameter panel. This allows users to observe the propagation pattern in a stepwise manner.

Identification of Contributing Nodes. By *contributing nodes*, we mean the nodes that lead to the coverage of a certain community or certain regions in the HoN. The contribution of a node n to a community c is measured by the number of nodes in c that are reached directly through n for the first time. The total contribution of a node n is the summation of its contributions to all communities. We choose to visualize twenty nodes with the highest total contributions using a stacked histogram. Each bin in the histogram corresponds to the coverage of one community. The bars with the same color correspond to the same contributing node. In Figure 4 (a) and (b), we show the subgraph before and after a critical tracing step. After that tracing step, the subgraph propagates to the upper part of the HoN. We can see that many nodes in the 8-th community are covered after this step, as indicated by the red arrow in Figure 4 (b). The node corresponding to the blue bars contributes most to the coverage of that community, as the blue bar in the 8-th bin is the tallest. By clicking on that blue bar, the contributing node is highlighted in yellow and the nodes

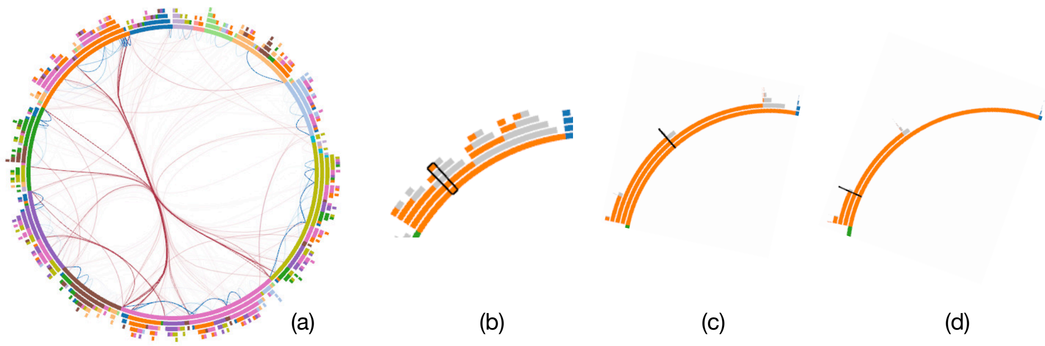

Fig. 5. The aggregation view. (a) Exact grouping using eco-realms. (b) to (d) The eco-realm of "Temperate Northern Pacific" with coarse grouping. (b) Uniform node weight. (c) Nodes are weighted by the number of original nodes. (d) Nodes are weighted by the number of ships. The same aggregated node is highlighted in black in (b) to (d).

reached from it are highlighted in blue in the subgraph. This indicates that the contributing node is an important transit point for the ships to propagate into the 8-th community. By identifying such nodes, domain experts can devise targeted species control strategies at certain critical ports to maximize the effectiveness and minimize the cost.

5.3 Aggregation View

The aggregation view provides an overview of the higher-order dependencies among groups of ports and their connections, corresponding to the design requirement **R2**. It also serves as a convenient interface to select the higher-order nodes with desired properties, e.g., the fifth-order nodes that contain ports in different eco-realms. The aggregation can be performed on the entire HoN or synchronized with the subgraph under expansion based on port grouping. The aggregated node corresponding to an original higher-order node is determined by converting each port associated with the higher-order node to the group containing that port. Formally, denoting a k-th-order node as a sequence of ports $\mathbf{n_i} = [p_{i_0}|p_{i_1}, \ldots, p_{i_{k-1}}]$, where p_{i_0} is the current port and $p_{i_1}, \ldots, p_{i_{k-1}}$ are the previously visited ports, and the group of a port p as $G(p)$, the aggregated node corresponds to node $\mathbf{n_i}$ can be written as

$$A(\mathbf{n_i}) = [G(p_{i_0})|G(p_{i_1}), \ldots, G(p_{i_{k-1}})]. \tag{4}$$

The edges are aggregated accordingly by summing up the weights of edges corresponding to the same pair of aggregated nodes.

We group the ports according to their eco-realms. This means that the higher-order nodes containing sequences of ports are aggregated into the higher-order nodes containing sequences of eco-realms. The edges are aggregated to show the number of ships moving among the eco-realms. Twelve groups of ports (i.e., eleven marine eco-realms and one group containing all freshwater ports) are considered. Unlike the original nodes, where two consecutive ports are always distinct, an aggregated node may contain two consecutive appearances of the same eco-realm, meaning that the ships move from one port to another in the same eco-realm. This will be effective for domain experts to distinguish the higher-order dependencies inside each eco-realm and among the eco-realms, which is critically important to the study of species invasion.

Coarse Grouping Aggregation. In some cases, the aggregation technique with the above *exact grouping* may not be necessary. For example, users may be interested in the higher-order nodes whose previous steps contain ports in other eco-realms without caring exactly what those eco-realms are. In other words, it suffices to distinguish the ports in the same eco-realm as the current port and the ports in different eco-realms. To accommodate this need, we further design an aggregation scheme with *coarse grouping*. With coarse grouping, the aggregated nodes can still be generated using Equation (4) but with a slightly different grouping function $G(p)$. Unlike the exact grouping function that always maps a port to a group, the coarse grouping function either maps a port to the group representing the eco-realm of the current port, or to a special status indicating that the port is in a different eco-realm. For example, the node [Singapore|Port Klang, Shanghai] will be aggregated into [Central Indo-Pacific|Central Indo-Pacific, Temperate Northern Pacific] with exact grouping but [Central Indo-Pacific|Central Indo-Pacific, Different Eco-realm] with coarse grouping. In our experiment, the number of aggregated nodes reduces from 396 to 180 with coarse grouping, allowing users to focus more on the between-group dependencies. Users can switch between exact grouping and coarse grouping depending on their needs.

Network Layout. We show the aggregation view using the circular layout, where the nodes are aligned on a circle and their connections are displayed inside the circle. The edges among nodes belonging to the same current group are colored in blue, while the edges among nodes belonging to different current groups are colored in brown. We bundle the edges for visual clarity using the force-directed edge bundling algorithm [15]. An aggregated node covers a sector of the circle, as highlighted by the black rectangle in Figure 5 (b). The number of layers in the sector represents the node's order, and the color of a layer represents the group of ports (i.e., eco-realm). The groups of ports are visited in the order from the outermost layer to the innermost layer (i.e., the current group is in the innermost layer). The gray color is reserved for the special group "different eco-realm". For example, the aggregated node highlighted in Figure 5 (b) exhibits five layers, from outermost to innermost, colored in orange, gray, gray, orange, and orange, respectively. This indicates that the node is fifth-order and the ships visited different eco-realms two and three steps before. The nodes are ordered according to their corresponding sequences of groups. That is, the nodes belonging to the same current group occupy a consecutive sector at the innermost layer, and then the nodes belonging to the same previous group are organized consecutively at the second inner layer, and so on. In Figure 5 (b), we can see that the nodes corresponding to the orange group are placed together. The second inner layer shows orange on the left side and gray on the right side, indicating that the nodes with the same previous group are on the left side and the nodes with different previous groups are on the right side.

The arc length of the sector is decided by the weight of the corresponding node. We provide three types of node weights. Figure 5 (b) shows the orange group with the uniform weight, where each node occupies the same arc length so that different nodes can be distinguished more easily. In Figure 5 (c), the aggregated nodes are weighted by the number of original nodes contained in them. We can observe from the arc lengths that most higher-order nodes exist among ports in the same eco-realm. In Figure 5 (d), the aggregated nodes are weighted by the number of ships related to each node. We observe that about half of the sector shows higher-order dependencies, within which a large proportion of ships travel within the same eco-realm, while a small proportion may bring in invasive species from other eco-realms, suggesting targeted control opportunities. A complete picture of the aggregation view with coarse grouping can be found in Figure 3 (d). Figure 5 (a) shows the aggregation view with exact grouping. Although it provides more details, it is more difficult to interpret as an overview due to its complexity.

5.4 Extension for Dynamic HoNs

When the higher-order dependencies change over time, a single HoN is incapable of capturing their dynamic behaviors. In order to accommodate the need for exploring dynamic HoNs, we extend

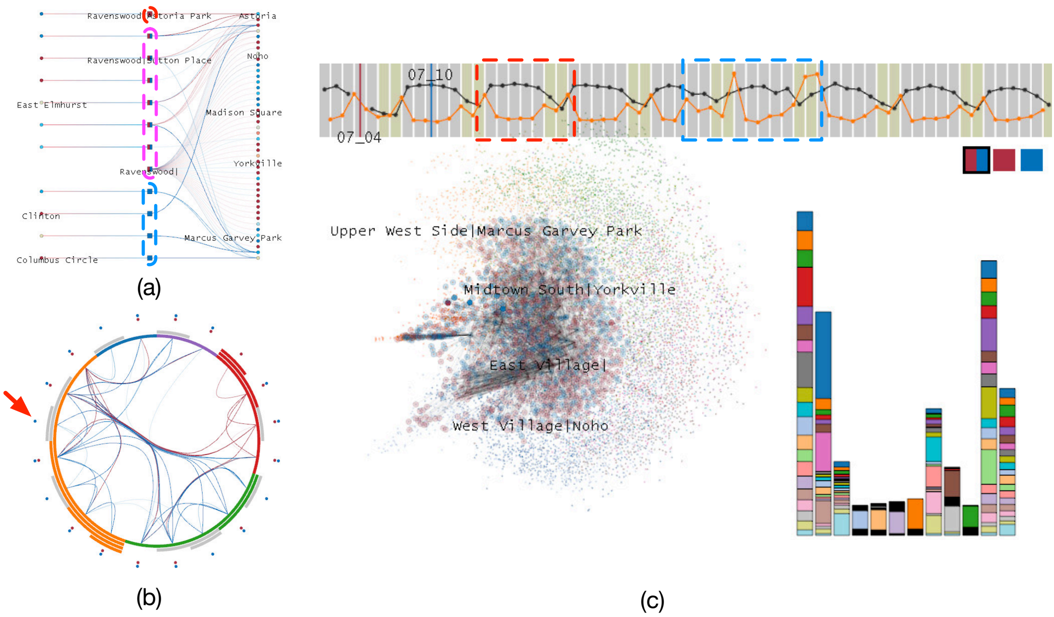

Fig. 6. Comparing two HoNs constructed using the New York City taxi trip data on Jul 4 (red) and Jul 10 (blue). (a) Individual node comparison with the POI (Ravenswood) selected. (b) Aggregated node comparison. (c) Subgraph comparison by tracing two steps forward the higher-order nodes related to Ravenswood.

the aforementioned framework to compare and understand multiple HoNs, fulfilling the design requirements **R5** and **R6**.

Time Slider and Overall Difference. Our framework divides the input sequential data into T time windows and produces a series of HoNs $G = [G_1, \ldots, G_T]$, where a network $G_i = \{V_i, E_i\}, i \in [1, T]$ encodes the higher-order dependencies in the i-th time window. A time slider is displayed for users to select a HoN for exploration or two HoNs for comparison. The selected HoNs are indicated by the red bar and an optional blue bar. We will use the red or blue HoN to refer to the HoN specified by the red or blue bar. On top of the time slider, two line plots visualize the overall difference among the HoNs. The orange curve shows the difference between each pair of neighboring HoNs, and the black curve shows the difference between a HoN and the red HoN currently under inspection.

The overall difference $\mathcal{D}(G_i, G_j)$ between two networks G_i and G_j is quantified by the *weight distance* [29] as

$$\mathcal{D}(G_i, G_j) = \frac{\sum u, v \in V_i \cup V_j \frac{w_{E_i}(u,v) - w_{E_j}(u,v)}{\max(w_{E_i}(u,v), w_{E_j}(u,v))}}{|E_i \cup E_j|}, \quad (5)$$

where $w_{E_i}(u, v)$ and $w_{E_j}(u, v)$ are the weights of edge (u, v) in G_i and G_j, respectively. If any of the nodes u and v or the edge (u, v) do not exist in one network, we simply consider the edge weight to be zero.

Dependency Comparison. We use the dependency view to compare the higher-order nodes in the two HoNs that are related to the same first-order node. The higher-order nodes are ordered according to their affiliation to the two HoNs. In addition, for each higher-order node, we display a single box to indicate this affiliation relationship. An example is shown in Figure 6 (a). From top to bottom, the higher-order nodes related to only the red HoN (indicated by red boxes), both HoNs (indicated by red/blue boxes), and the blue HoN (indicated by blue boxes) are shown. We color a box with its left part in red and its right part in blue to indicate that the corresponding node belongs to both HoNs. Furthermore, the edge color is used to indicate the difference of transition probabilities corresponding to that edge in the two HoNs. The edge is blue if the transition probability in the blue HoN is higher; otherwise, it is red. The transparency is determined by the absolute difference. A more opaque edge indicates a larger absolute difference.

Aggregation Comparison. We use the aggregation view to compare the higher-order dependencies among groups of nodes in the two HoNs. Two circles beyond the outer ring of an aggregated node are used to indicate whether or not the node exists in the two networks. A red circle is displayed if the aggregated node exists in the red HoN, and a blue circle is displayed if otherwise. An example is shown in Figure 6 (b). We find that most aggregated nodes exist in both HoNs as both circles are displayed. There are still several aggregated nodes that only belong to one HoN. For example, the aggregated node [orange|gray, gray] pointed by the red arrow only exists in the blue HoN as only the blue circle is displayed. This indicates that the taxis visiting two other regions before arriving at the orange one form higher-order dependencies in the blue HoN but not in the red HoN. Users can select an aggregated node to view its corresponding higher-order nodes in the dependency view for detailed comparison. Similar to edge coloring in the dependency view, edge colors in the aggregation view represent the difference of aggregated transition probabilities.

Propagation Comparison. We use the subgraph view to compare the propagation patterns on the two HoNs, as shown in Figure 6 (c). The propagation is traced from the selected higher-order nodes in each individual HoN. A red circle is displayed over a higher-order node if that node is more likely to be visited on the red HoN, and a blue circle is displayed if otherwise. Similarly, the opacity of a circle indicates the probability difference. The stacked histogram on the right still shows the nodes with the highest contributions. To identify the most influential nodes, we use the contribution of a node which is defined as the summation of its contributions in the two HoNs. Three legends are displayed on the upper-right corner to allow switching among the comparison of two HoNs, the red HoN, and the blue HoN.

6 CASE STUDY ON SPECIES INVASION VIA GLOBAL SHIPPING NETWORK

The global ship movement data are made available by the Lloyd's List Intelligence, which contains more than two thirds of active ships globally (measured in dead weight tonnages). The raw data contain 3,415,577 individual ship voyages corresponding to 65,591 ships that move among 4,108 ports globally between May 1, 2012 and April 30, 2013. The data also contain metadata of ships, such as ship type, voyage start and end time, ship size, as well as metadata of ports such as coordinates and country. The environmental conditions (temperature and salinity) of ports are obtained from the Global Ports Database [20] and the World Ocean Atlas [3, 23]. The eco-region information comes from Marine Ecoregions of the World [30] and Freshwater Ecoregions of the World [2]. Ports (and associated ship movements) that have corresponding coordinates, eco-region and environmental conditions are retained for analysis.

6.1 Domain Experts' Workflow and Insights

Locating Ports with Higher-Order Dependencies (R1). The experts wanted to investigate potential species invasions from South America to Europe via global shipping, and evaluate the influence of higher-order movement patterns of shipping. As shown in Figure 7 (a), the experts first used the geographic view to zoom in to South America. To identify ports through which ships demonstrate higher-order movement patterns, the experts chose to color the ports by the number

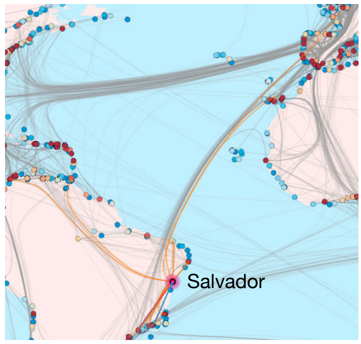

(a)

Ports	#HO Nodes
Suape	19
Vitoria	19
Salvador	13
Tubarao	6
Praia Mole	5
Portocel	2
Ponta do Ubu	2
Aratu	2
Recife	2
Madre de Deus	1
Cabedelo	1
Ilheus	1
Maceio	1
Jubarte Field	1

(b)

Fig. 7. Identifying a port of interest. (a) The port Salvador in Brazil is highlighted with a magenta halo in the geographic view. (b) The nearby ports are listed in the table view ordered by their numbers of associated higher-order nodes.

of higher-order dependencies, and focused on ports shown in red (the ones that demonstrate the most higher-order dependencies). The number of candidate ports is thus reduced from hundreds to tens. The experts then simply clicked on the area of interest, and in the table view (Figure 7 (b)), the ports in the area were sorted by the number of higher-order dependencies. The experts clicked through the top ports to highlight shipping paths from those ports, and quickly identified Salvador in Brazil, which shows a direct connection in the bundle from South America to Europe.

Exploring Higher-Order Dependencies (R3). The experts then evaluated how the movement pattern from Salvador is influenced by from where the ships came to Salvador. After selecting Salvador in the table view, all its higher-order dependencies are displayed in the dependency view (Figure 8 (c)). At a glance, the experts knew that without knowing a ship's previous locations, the ship's next step from Salvador is uncertain. This is revealed by both the weak connections (dimmed visually) from the first-order node [Salvador|] (highlighted by the blue arrow in Figure 8 (c)) to all 16 potential destination ports on the right, and the white entropy box of [Salvador|] (high entropy indicating low certainty). A quick drag-and-drop selection of the destination ports reveals that the ships from Salvador are mainly container carriers (UCC), and shipping at Salvador remains active throughout the year (Figure 8 (b)).

Following the link from Rio de Janeiro to the second-order node [Salvador|Rio de Janeiro] (highlighted by the red arrow in Figure 8 (c)), the experts discovered that knowing ships came from Rio de Janeiro to Salvador does not significantly influence the ships' choices for the next step, indicated by the light red KLD box (meaning low difference compared with the distribution from the first-order node), and the light blue entropy box (indicating low certainty). Essentially, this implies that *the second order is insufficient in capturing the complex dependencies in this case.* It is likely that Rio de Janeiro, being the second largest city of Brazil, has a port so versatile and provides limited information in narrowing down complex ship movement patterns. The reason that the second-order node [Salvador|Rio de Janeiro] is included in HoN is that it bridges connections from other essential higher-order nodes.

The experts then proceeded to explore dependencies beyond the second order. By selecting the fourth-order path Salvador → Santos → Rio de Janeiro → Salvador, as highlighted in Figure 8 (c), the experts observed a *loop*, that if a ship has been observed following the loop at least once, the ship will keep following the loop for sure. The dark blue entropy box and dark red KLD box at port

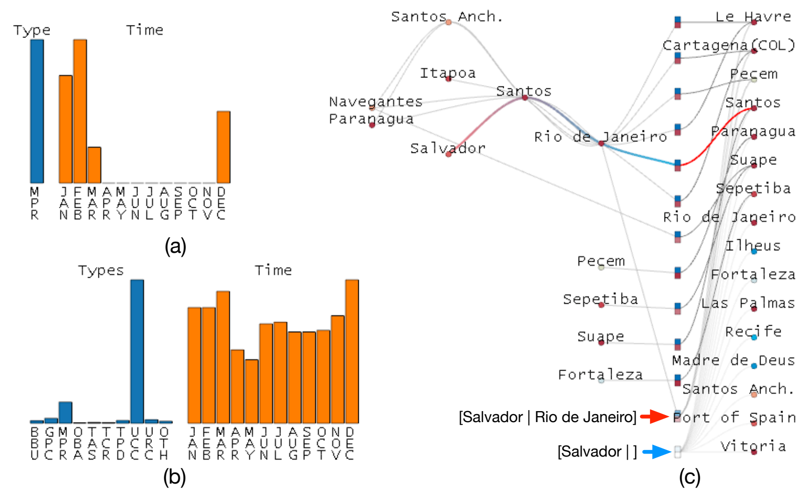

Fig. 8. The higher-order dependencies related to Salvador. (a) Histograms of ship types and temporal activities of fourth-order movement patterns from Salvador. (b) Histograms of ship types and temporal activities for all ships from Salvador. (c) Higher-order dependencies related to Salvador in the dependency view.

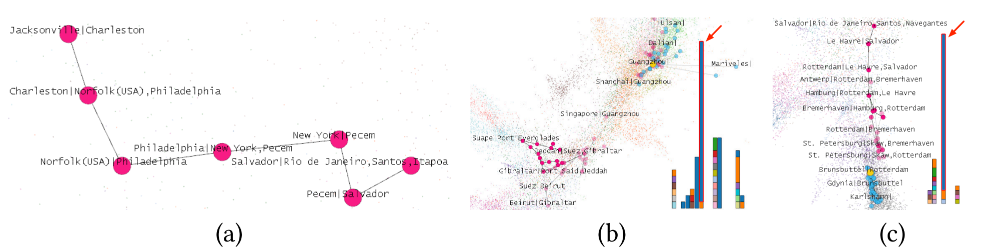

Fig. 9. (a) Tracing how the species may propagate from Salvador in a stepwise manner. (b) The propagation eventually influences multiple ports in East Asia, which are far away from Salvador. (c) Another direction of the propagation covers multiple ports in Northwest Europe.

[Salvador|Rio de Janeiro, Santos, Salvador] indicate that this pattern displays high certainty and is significantly different than the first-order movement pattern. Moreover, the bar charts (Figure 8 (a)) in the dependency view show that ships following this fourth-order pattern are exclusively cruise ships (MPR) and are only active in the summer (December to March in the South Hemisphere), *revealing the underlying reason behind this higher-order dependency.*

Exploring the Influence of Higher-Order Dependencies in Propagation (R4). The experts further explored how higher-order dependencies influence the propagation of invasive species via shipping. Specifically, knowing that the ships came from Itapoa or Navengates before sailing through Santos and Rio de Janeiro to Salvador, the experts wanted to figure out how the species propagate differently. The experts first selected the fourth-order pathway Itapoa → Santos → Rio de Janeiro → Salvador in the dependency view, and the corresponding node [Salvador|Rio de Janeiro, Santos, Itapoa] is automatically selected in the subgraph view. The experts clicked "Trace" button to see how the species may propagate from the given port in a stepwise manner. As shown in Figure 9 (a), the species first went to Pecem in Brazil and then to New York City in USA.

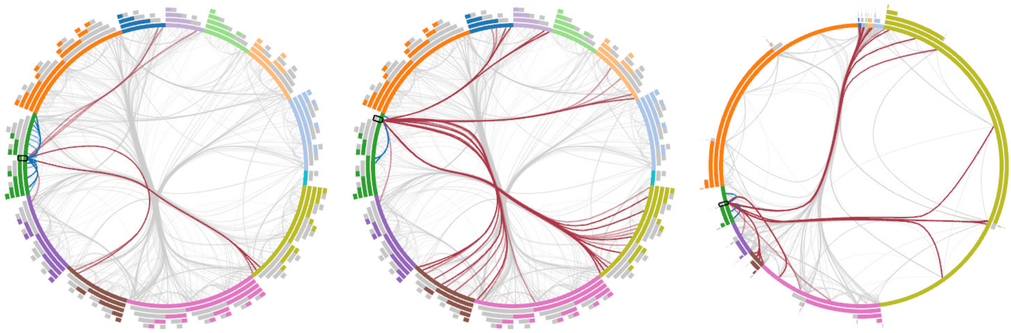

(a) (b) (c)

Fig. 10. Investigating higher-order dependencies at different granularities. (a) Studying a sector which both the current and previous ports are in the Tropical Atlantic eco-realm. (b) Studying a sector which the current ports are in the Tropical Atlantic eco-realm, but the previous ports are not. (c) Changing the view in (b) from uniform node weight to weighted by the number of ships.

After that, with high certainty, the species were propagating toward the blue cluster on the left, which mainly consists of ports in Northeast America. After tracing a few more steps, the possible diffusion diverged. A branch kept propagating in Northeast America with high certainty. More interestingly, the species may influence multiple ports in East Asia, represented as the green cluster at the top-right corner as shown in Figure 9 (b), which was topologically far from the initial port Salvador on the lower left. The experts noticed the new spike in the stacked histogram, consisting mainly of a single color (blue). This indicates that a port is making significant contribution to the massive dispersion of species in that cluster. The experts clicked on the dominating blue bar of that spike, and the subgraph view reveals that Guangzhou was the port that facilitated the potential massive spread of invasive species in East Asia. *Knowing that Guangzhou is the entry point to species spreading in that region is vital when developing targeted invasive species control strategies* to prevent Brazilian species from invading East Asia. Tracing back, Guangzhou was invaded by ships sailing from Gibraltar through the Mediterranean Sea, then through the Suez Canal to the Red Sea, passing Jeddah and finally to Guangzhou. These ports on the shipping path also deserve close monitoring.

On the contrary, when the experts selected the pathway Navengantes → Santos Arch → Santos → Rio de Janeiro → Salvador in the dependency view, with high certainty the species will propagate toward the gray cluster at the bottom as shown in Figure 9 (c), which mainly consists of ports in Northwest Europe. The port leading to the mass diffusion in the cluster was Brunsbuttel. Through the interactive exploration and comparison, the experts gained a comprehensive understanding on how the higher-order dependencies may influence the subsequent propagation.

Exploring Higher-Order Dependencies at Different Granularities (R2). Finally, the experts wanted to explore the connections at a higher level: the *eco-realm* is the largest biogeographic division of the sea [30]; species coming from other eco-realms are more likely to be non-indigenous and will incur invasions. The question is: how do the connections differ whether the previous port was also in the Tropical Atlantic eco-realm (which Salvador is in) or was in a different eco-realm? The experts first chose to color the ports in the geographic view with eco-realms. Tropical Atlantic was colored dark green. Then the experts shifted to the aggregation view, and chose the sector which both the current and previous ports are in the Tropical Atlantic eco-realm. The sector is denoted by two layers of dark green, as shown in Figure 10 (a). The aggregation view reveals ampler and stronger intra-eco-realm connections as denoted by blue links, compared with inter-eco-realm

Fig. 11. Comparison of PageRank risk simulation on the FoN and the HoN. Blue ports are risks overestimated on the FoN and red ports are risks underestimated on the FoN.

connections as denoted by brown links (mainly connections to Temperate Southern Africa, Temperate Northern Atlantic, and Temperate South America). By cross-checking with ship types in the dependency view, the experts found out that variable types of ships exist for this case.

On the contrary, when the experts chose the sector which the current ports are in Tropical Atlantic but the previous ports are not (the sector denoted by the innermost layer as dark green and the outer layer as gray, as shown in Figure 10 (b)), the inter-eco-realm connections are stronger, including additional connections to Tropical Eastern Pacific and Central Indo-Pacific. Meanwhile, the dependency view suggested that these inter-eco-realm navigation patterns were exclusively made by container carriers. The experts came to the preliminary conclusion that *ships coming from different eco-realms were more likely to keep traveling among eco-realms, posing higher risks of bringing in non-indigenous species*. Furthermore, in terms of species management strategies for specific types of ships, *container carriers posed the highest risk for the introduction of non-indigenous species*.

Last, the experts changed the widths of sectors from uniform to the number of ships, as shown in Figure 10 (c), which gives an intuitive overview of the composition of all higher-order dependencies. The experts noticed that although ships coming from other eco-realms to Tropical Atlantic have higher chances of keeping with the inter-eco-realm voyages, the number of inter-eco-realm trips was much less than that of intra-eco-realm trips. The fact that the more risky inter-eco-realm voyages were the minorities suggested that *targeted species control policies only need to focus on a small fraction of ships and routes*.

Insights Revealed by HoNVis at the Global Scale. HoNVis not only enables interactive exploration as shown in the above use case, but also reveals the influence of higher-order dependencies at the global scale. For example, one observation was for ports in the Arctic. The change of climate had been melting the Arctic sea ice at an alarming speed and opening up Arctic shipping routes [12]. Therefore, there are growing concerns on threats to the valuable resources in the Arctic posed by invasive species via the unprecedented growth of shipping. The PageRank algorithm naturally simulates the flow of species hitchhiking onto ships, with random resets accounting for the changing or unobserved shipping activities. The PageRank score of each port indicates the relative risk that species will end up to the port in multiple steps. The PageRank risk estimation on the FoN marks multiple ports in the Arctic as high risk, but as pointed out in Section 3, the HoN can improve the result of PageRank running upon. Surprisingly, the estimated risks for Arctic ports were overwhelmingly overestimated on the FoN. This is indicated by the ports in blue as shown in Figure 11. For example, the PageRank score of Murmansk, a major Arctic port in Russia, was 4.52×10^{-4} on the FoN, but only 1.57×10^{-4} on the HoN. The dependency view suggested that by using the HoN, traffic from hub ports such as Rotterdam to the Arctic ports is more likely to go back immediately to those hub ports rather than moving randomly among Arctic ports. Thus the relative flow of species in the Arctic is smaller on HoN. The information on the overestimation of risks made possible by HoNVis is important for policy makers.

7 CASE STUDY ON NEW YORK CITY TAXI TRIPS

We analyze the New York City taxi trips to study the dynamic behaviors of HoNs. The taxi trip data were collected by NYC Taxi & Limousine Commission (TLC) and are made available by Whong [33]. The raw data contain 173,179,759 individual trips carried by 14,144 yellow taxis in New York City between January 1 and December 31, 2013. For each trip, the pick-up and drop-off dates and locations are recorded. The trips on the same day are used to construct the HoN on that day. We present our case study using two sets of dates and their corresponding HoNs.

7.1 Exploration of HoNs in July and August 2013

Observing the Dynamic Behaviors of HoNs (R5). We first investigate the overall dynamic patterns of HoNs during July and August 2013. In Figure 6 (c), the neighboring HoNs comparison (orange curve) demonstrates a pattern repeating stably in the weekly period. Note that the background of weekends is colored differently from that of weekdays. The red dashed box highlights a typical period of this weekly pattern. We can see clearly that the difference between a weekday and a weekend is larger than the difference between two weekdays, resulting in a spike on the orange curve. Over each weekend, we can normally identify two consecutive spikes (between Friday and Saturday, and between Sunday and Monday) and a trough between them due to the small difference between Saturday and Sunday.

We also find two abnormal patterns in this two months. The first one is on July 4 (the Independence Day) and the second covers the beginning of August (as highlighted in the blue dashed box). We focus on the HoN on July 4 here and will discuss the second anomaly in Section 7.2. By selecting July 4 to investigate, the black curve compares the HoN on July 4 to the other HoNs. We can see that July 4 is more similar to the weekends than the weekdays, although the difference between July 4 is still slightly larger than those between two consecutive weekends. These results confirm that the weight distance between HoNs can effectively capture the overall difference of travel patterns through taxis.

Comparing HoNs (R6). We then investigate the difference between the HoN on the Independence Day (July 4) and a normal weekday (July 10). In Figure 6 (b), the aggregation view demonstrates the difference at the borough level. We find that two types of probability transitions are higher in the red HoN: the transitions within Manhattan (the orange sectors) and those between Queens and other boroughs. This indicates that, *during holidays, people are more likely to travel within Manhattan for tourism or between Queens and other boroughs, probably transporting from the JFK airport and other locations through taxis.*

However, we are not able to conclude that starting from a POI in Manhattan, a taxi is more likely to stay in the borough, when individual POIs are investigated. For example, we select Ravenswood, a POI with a moderate number of higher-order nodes. In Figure 6 (a), the dependency view shows that the higher-order nodes corresponding to Ravenswood are similar in the two HoNs, sharing seven nodes among the twelve ones. In Figure 6 (c), the subgraph view further shows that tracing the corresponding higher-order nodes two steps on the two HoNs leads to a balanced distribution over all higher-order nodes as similar numbers of red and blue circles are shown. We can confirm with the geographic view that similar POIs are reached on the two HoNs.

7.2 Exploration of HoNs on Sundays in 2013

Observing the Dynamic Behaviors of HoNs (R5). When consecutive days are investigated, the difference between the weekdays and weekends usually dominates the difference between neighbors. In this section, we focus on the difference between the neighboring HoNs constructed from all Sundays in 2013. In Figure 12 (e), we can see that the neighboring Sundays are mostly

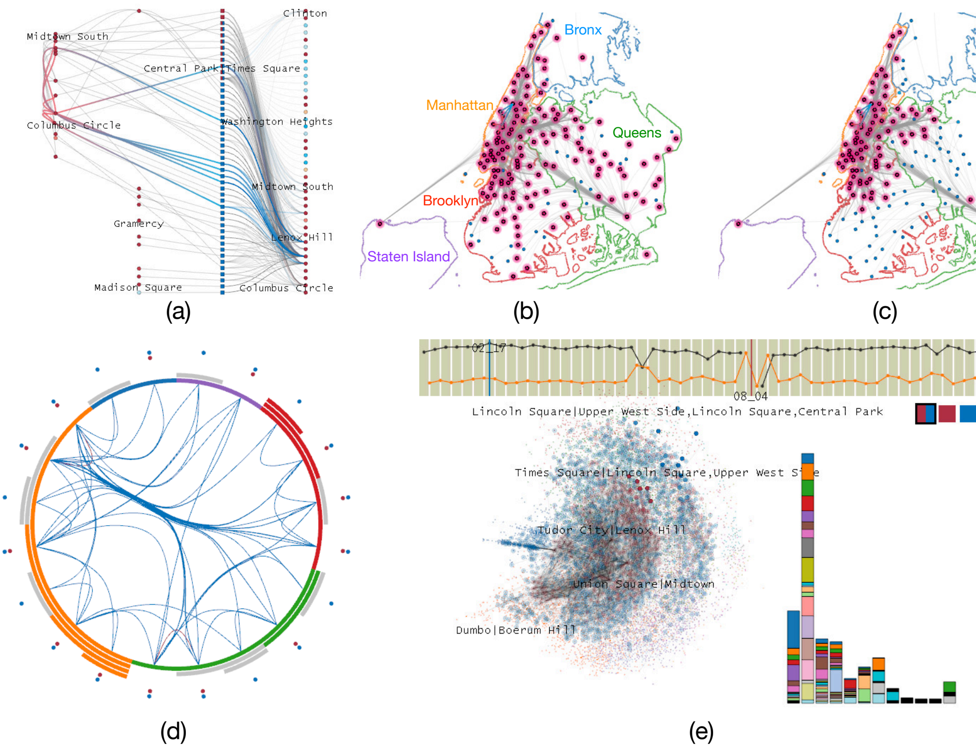

Fig. 12. Comparing HoNs constructed from the New York City taxi trips on all Sundays in 2013. Two HoNs on Feb 17 (blue) and Aug 4 (red) are selected for comparison. (a) Individual node comparison with Central Park selected as the current POI and Times Square as a previous POI. (b) and (c) The POIs reached in three steps by tracing the higher-order nodes shown in (a) on Feb 17 and Aug 4, respectively. (d) Aggregated node comparison. (e) Subgraph comparison by tracing three steps forward the higher-order nodes related to Central Park.

similar as the orange curve is flat in most of the periods. However, three spikes can be found as well: one lower spike appears on May 26 and two higher consecutive spikes exist on Aug 4 and Aug 11. Since May 26 is the Memorial Day weekend in 2013 (May 27 is the Memorial Day) with many events scheduled, it is reasonable that people may have a different travel pattern than an ordinary weekend. On Aug 4, its corresponding HoN is highly different from all the others except the one on Aug 11, as shown by the black curve in Figure 12 (e). This is consistent with the abnormal pattern highlighted in the blue dashed box in Figure 6 (c). With further investigation, we suspect that this anomaly relates to Boro Taxis [1] introduced to New York City in August 2013.

Comparing HoNs (R6). We first study how the travel patterns on Aug 4 differ from those on the ordinary days. Two HoNs are compared: the HoN on Aug 4 (red) and the HoN on Feb 17 (blue). In Figure 12 (d), the aggregation view shows that among the 20 aggregated nodes, the blue HoN has seven nodes of its own and shares the other 13 with the red HoN. This means that the blue HoN exhibits more patterns of higher-order dependencies. In addition, the blue HoN also has higher aggregated transition probabilities between most aggregated nodes, as suggested by the blue edges. The only two red edges are found corresponding to trips inside Manhattan and Queens. The raw data confirms that the yellow taxis were less active during this anomaly. Only 5,927 taxis were recorded on Aug 4, which is much smaller than the total number of yellow taxis (14,144) and the minimum number of taxis on the other days (10,953 on Dec 25, Christmas Day). In addition, the number of trips (202,310) is much smaller than the daily average in this year (474,465) as well.

This trend can be observed at individual POIs as well. In Figure 12 (a), we select Central Park in Manhattan for exploration. While 47 higher-order nodes appear in the two HoNs, only 12 are found in the red HoN, among which ten are shared with the blue HoN. By further choosing Times Square as a previous POI, we find that one second-order node [Central Park|Times Square] is related to both HoNs, and the other six nodes correspond to only the blue one. By tracing these nodes three steps forward, the subgraph view shows that most nodes are blue, indicating higher probabilities for them to be visited on the blue HoN. There are fewer nodes colored in red, and most of them are close to the center of the subgraph, where most of the first- and second-order nodes reside in. Figure 12 (b) and (c) show the POIs corresponding to the tracing results on the blue and red HoNs, respectively. We can see that the resulting POIs cover a much narrower area (mostly Manhattan) on Aug 4, which further confirms our finding using the aggregation view. Given that Boro Taxis are not allowed to pick up passengers in the south of Manhattan including Central Park, the introduction of Boro Taxis is likely the cause of this anomaly.

8 CONCLUSIONS AND FUTURE WORK

We have presented HoNVis, a visual analytics framework for visualizing and exploring higher-order networks. We focus on two real-world applications and work closely with domain experts in network science and marine ecology to compile the task list and define design requirements. Our HoNVis design leverages five linked views to enable users to explore the HoN at different levels of detail and investigate higher-order dependencies among higher-order nodes. By directly contrasting the HoN and its FoN counterpart and visualizing higher-order dependencies, we tackle the key challenges in visualizing higher-order dependencies in networks, which is a milestone in pushing the understanding of the formation and impact of higher-order dependencies. The efficacy of HoNVis is demonstrated through results gathered by two domain experts who use the system to investigate species invasion in the global shipping network. Several critical insights that can only be obtained with the use of HoNVis are reported. In addition, we demonstrate that HoNVis is useful to reveal the dynamic behaviors using the New York City taxi trips.

We acknowledge the limitations of the current version of HoNVis, including the lack of effective visual hints to aid the users in navigating through the different views, and the challenge of labeling when the data are large. We advocate the idea of automatically producing statistics of all possible dependency structures (such as large loops) and aiding in the identification of principal patterns, which is a non-trivial task given the computational complexity.

Besides the two applications presented in this paper, the framework of HoNVis can be generalizable to other types of HoNs, which we plan to implement in the near future. For example, given that air transportation exhibits higher-order dependencies [28], HoNVis can help to explore epidemic outbreak scenarios through domestic and international travels, by substituting ships with airplanes and invasive species with contagious diseases. Similarly, HoNVis can also help to explore information diffusion patterns through phone call or online activities in social networks, by treating phone call or retweet cascades as ship trajectories.

ACKNOWLEDGEMENTS

This work was supported in part by the U.S. National Science Foundation through grants IIS-1456763, IIS-1455886, ACI-1029584, DEB-1427157, CNS-1629914, and the U.S. Army Research Laboratory under Cooperative Agreement No. W911NF-09-2-0053.

REFERENCES

[1] Boro Taxis. https://en.wikipedia.org/wiki/Boro_taxi.

[2] R. Abell, M. L. Thieme, C. Revenga, et al. Freshwater ecoregions of the world: A new map of biogeographic units for freshwater biodiversity conservation. *BioScience*, 58(5):403–414, 2008.

[3] J. I. Antonov, D. Seidov, T. P. Boyer, R. A. Locarnini, A. V. Mishonov, H. E. Garcia, O. K. Baranova, M. M. Zweng, and D. R. Johnson. *World Ocean Atlas 2009, Volume 2, Salinity.* U.S. Government Printing Office, 2010.

[4] G. Bagler. Analysis of the airport network of India as a complex weighted network. *Physica A: Statistical Mechanics and its Applications*, 387(12):2972–2980, 2008.

[5] J. Blaas, C. Botha, E. Grundy, M. Jones, R. Laramee, and F. Post. Smooth graphs for visual exploration of higher-order state transitions. *IEEE Transactions on Visualization and Computer Graphics*, 15(6):969–976, 2009.

[6] V. D. Blondel, J.-L. Guillaume, R. Lambiotte, and E. Lefebvre. Fast unfolding of communities in large networks. *Journal of Statistical Mechanics: Theory and Experiment*, 2008(10):P10008, 2008.

[7] P. Bodesinsky, B. Alsallakh, T. Gschwandtner, and S. Miksch. Exploration and assessment of event data. In *Proceedings of EuroVis Workshop on Visual Analytics*, 2015.

[8] Y. Chen, P. Xu, and L. Ren. Sequence synopsis: Optimize visual summary of temporal event data. *IEEE Transactions on Visualization and Computer Graphics*, 24(1):45–55, 2018.

[9] F. Chierichetti, R. Kumar, P. Raghavan, and T. Sarlos. Are web users really Markovian? In *Proceedings of International Conference on World Wide Web*, pages 609–618, 2012.

[10] J. M. Drake and D. M. Lodge. Global hot spots of biological invasions: Evaluating options for ballast-water management. *Proceedings of the Royal Society of London B: Biological Sciences*, 271(1539):575–580, 2004.

[11] F. Du, B. Shneiderman, C. Plaisant, S. Malik, and A. Perer. Coping with volume and variety in temporal event sequences: Strategies for sharpening analytic focus. *IEEE Transactions on Visualization and Computer Graphics*, 23(6):1636–1649, 2017.

[12] B. Ellis and L. Brigham. *Arctic Marine Shipping Assessment 2009 Report.* Arctic Council's Protection of the Arctic Marine Environment (PAME), 2009.

[13] N. Ferreira, J. Poco, H. T. Vo, J. Freire, and C. T. Silva. Visual exploration of big spatio-temporal urban data: A study of New York City taxi trips. *IEEE Transactions on Visualization and Computer Graphics*, 19(12):2149–2158, 2013.

[14] D. Guo. Flow mapping and multivariate visualization of large spatial interaction data. *IEEE Transactions on Visualization and Computer Graphics*, 15(6):1041–1048, 2009.

[15] D. Holten and J. J. van Wijk. Force-directed edge bundling for graph visualization. *Computer Graphics Forum*, 28(3):983–990, 2009.

[16] X. Huang, Y. Zhao, C. Ma, J. Yang, X. Ye, and C. Zhang. TrajGraph: A graph-based visual analytics approach to studying urban network centralities using taxi trajectory data. *IEEE transactions on visualization and computer graphics*, 22(1):160–169, 2016.

[17] International Maritime Organization. *International Shipping Facts and Figures - Information Resources on Trade, Safety, Security, Environment*, 2012.

[18] M. Jacomy, T. Venturini, S. Heymann, and M. Bastian. ForceAtlas2, a continuous graph layout algorithm for handy network visualization designed for the Gephi software. *PLoS ONE*, 9(6):e98679, 2014.

[19] P. Kaluza, A. Kölzsch, M. T. Gastner, and B. Blasius. The complex network of global cargo ship movements. *Journal of the Royal Society Interface*, 7(48):1093–1103, 2010.

[20] R. P. Keller, J. M. Drake, M. B. Drew, and D. M. Lodge. Linking environmental conditions and ship movements to estimate invasive species transport across the global shipping network. *Diversity and Distributions*, 17(1):93–102, 2011.

[21] S. Kullback and R. A. Leibler. On information and sufficiency. *The Annals of Mathematical Statistics*, 22(1):79–86, 1951.

[22] Z. Liu, B. Kerr, M. Dontcheva, J. Grover, M. Hoffman, and A. Wilson. CoreFlow: Extracting and visualizing branching patterns from event sequences. *Computer Graphics Forum*, 36(3):527–538, 2017.

[23] R. A. Locarnini, A. V. Mishonov, J. I. Antonov, T. P. Boyer, H. E. Garcia, O. K. Baranova, M. M. Zweng, and D. R. Johnson. *World Ocean Atlas 2009, Volume 1: Temperature.* U.S. Government Printing Office, 2010.

[24] S. Malik, B. Shneiderman, F. Du, C. Plaisant, and M. Bjarnadottir. High-volume hypothesis testing: Systematic exploration of event sequence comparisons. *ACM Transactions on Interactive Intelligent Systems*, 6(1):9:1–9:23, 2016.

[25] J. L. Molnar, R. L. Gamboa, C. Revenga, and M. D. Spalding. Assessing the global threat of invasive species to marine biodiversity. *Frontiers in Ecology and the Environment*, 6(9):485–492, 2008.

[26] L. Page, S. Brin, R. Motwani, and T. Winograd. The PageRank citation ranking: Bringing order to the Web, 1999.

[27] C. Partl, S. Gratzl, M. Streit, A. M. Wassermann, H. Pfister, D. Schmalstieg, and A. Lex. Pathfinder: Visual analysis of paths in graphs. *Computer Graphics Forum*, 35(3):71–80, 2016.

[28] M. Rosvall, A. V. Esquivel, A. Lancichinetti, J. D. West, and R. Lambiotte. Memory in network flows and its effects on spreading dynamics and community detection. *Nature Communications*, 5, 2014.

[29] P. Shoubridge, M. Kraetzl, W. Wallis, and H. Bunke. Detection of abnormal change in a time series of graphs. *Journal of Interconnection Networks*, 3(01n02):85–101, 2002.

[30] M. D. Spalding, H. E. Fox, G. R. Allen, et al. Marine ecoregions of the world: A bioregionalization of coastal and shelf areas. *BioScience*, 57(7):573–583, 2007.

[31] M. Steptoe, R. Krüger, R. Garcia, X. Liang, and R. Maciejewski. A visual analytics framework for exploring theme park dynamics. *ACM Transactions on Interactive Intelligent Systems*, 8(1):4:1–4:27, 2018.

[32] T. von Landesberger, F. Brodkorb, P. Roskosch, G. Andrienko, N. Andrienko, and A. Kerren. MobilityGraphs: Visual analysis of mass mobility dynamics via spatio-temporal graphs and clustering. *IEEE Transactions on Visualization and Computer Graphics*, 22(1):11–20, 2016.

[33] C. Whong. FOILing NYC's Taxi Trip Data. https://chriswhong.com/open-data/foil_nyc_taxi/.

[34] K. Wongsuphasawat, J. A. G. Gómez, C. Plaisant, T. D. Wang, M. Taieb-Maimon, and B. Shneiderman. LifeFlow: Visualizing an overview of event sequences. In *Proceedings of ACM SIGCHI Conference*, pages 1747–1756, 2011.

[35] K. Wongsuphasawat and D. Gotz. Exploring flow, factors, and outcomes of temporal event sequences with the outflow visualization. *IEEE Transactions on Visualization and Computer Graphics*, 18(12):2659–2668, 2012.

[36] J. Xu, T. L. Wickramarathne, and N. V. Chawla. Representing higher-order dependencies in networks. *Science Advances*, 2(5):e1600028, 2016.

[37] J. Xu, T. L. Wickramarathne, N. V. Chawla, E. K. Grey, K. Steinhaeuser, R. P. Keller, J. M. Drake, and D. M. Lodge. Improving management of aquatic invasions by integrating shipping network, ecological, and environmental data: Data mining for social good. In *Proceedings of ACM SIGKDD Conference*, pages 1699–1708, 2014.

[38] J. Zhang, H. Guo, and X. Yuan. Efficient unsteady flow visualization with high-order access dependencies. In *Proceedings of IEEE Pacific Visualization Symposium*, pages 80–87, 2016.

Received July 2018